

Ameloblastin Inhibits Cranial Suture Closure by Modulating Msx2 Expression and Proliferation

Phimon Atsawasuwan^{1,2}, Xuanyu Lu¹, Yoshihiro Ito¹, Youbin Zhang¹, Carla A. Evans², Xianghong Luan^{1,2*}

1 Brodie Laboratory for Craniofacial Genetics, Department of Oral Biology University of Illinois College of Dentistry, Chicago, Illinois, United States of America, **2** Department of Orthodontics University of Illinois College of Dentistry, Chicago, Illinois, United States of America

Abstract

Deformities of cranial sutures such as craniosynostosis and enlarged parietal foramina greatly impact human development and quality of life. Here we have examined the role of the extracellular matrix protein ameloblastin (Ambn), a recent addition to the family of non-collagenous extracellular bone matrix proteins, in craniofacial bone development and suture formation. Using RT-PCR, western blot and immunohistochemistry, Ambn was localized in mouse calvarial bone and adjacent condensed mesenchyme. Five-fold Ambn overexpression in a *K14*-driven transgenic mouse model resulted in delayed posterior frontal suture fusion and incomplete suture closure. Moreover, Ambn overexpressor skulls weighed 13.2% less, their interfrontal bones were 35.3% thinner, and the width between frontal bones plus interfrontal suture was 14.3% wider. Ambn overexpressing mice also featured reduced cell proliferation in suture blastemas and in mesenchymal cells from posterior frontal sutures. There was a more than 2-fold reduction of *Msx2* in Ambn overexpressing calvariae and suture mesenchymal cells, and this effect was inversely proportionate to the level of Ambn overexpression in different cell lines. The reduction of *Msx2* expression as a result of Ambn overexpression was further enhanced in the presence of the MEK/ERK pathway inhibitor O126. Finally, Ambn overexpression significantly reduced *Msx2* down-stream target gene expression levels, including osteogenic transcription factors *Runx2* and *Osx*, the bone matrix proteins *Ibsp*, *Coll*, *Ocn* and *Opn*, and the cell cycle-related gene *CcnD1*. Together, these data suggest that Ambn plays a crucial role in the regulation of cranial bone growth and suture closure via *Msx2* suppression and proliferation inhibition.

Citation: Atsawasuwan P, Lu X, Ito Y, Zhang Y, Evans CA, et al. (2013) Ameloblastin Inhibits Cranial Suture Closure by Modulating *Msx2* Expression and Proliferation. *PLoS ONE* 8(4): e52800. doi:10.1371/journal.pone.0052800

Editor: Chi Zhang, University of Texas Southwestern Medical Center, United States of America

Received: September 4, 2012; **Accepted:** November 21, 2012; **Published:** April 4, 2013

Copyright: © 2013 Atsawasuwan et al. This is an open-access article distributed under the terms of the Creative Commons Attribution License, which permits unrestricted use, distribution, and reproduction in any medium, provided the original author and source are credited.

Funding: This study has been generously supported by grant DE19155 from the National Institute of Dental and Craniofacial Research (<http://www.nidcr.nih.gov/>). The funders had no role in study design, data collection and analysis, decision to publish, or preparation of the manuscript.

Competing Interests: The authors have declared that no competing interests exist.

* E-mail: luan@uic.edu

Introduction

During skull development, calvarial bones expand from initial ossification centers toward the suture interface between adjacent bones [1]. Developmentally, this gradual intramembranous ossification is accomplished by the differentiation of ectomesenchymal cells into calvarial osteoblasts [2]. On a molecular level, membranous bone ossification is regulated by a number of growth and transcription factors as well as extracellular matrix proteins, including fibroblast growth factor receptors *FGFR1* and *FGFR2* [3], transcription factors *CBFA1/RUNX2* [4–6], *MSX2* [7], *TWIST* [8],[9], and matrix proteins osteopontin and tenascin [10],[11]. Abnormal changes in these factors not only affect bone thickness and mineralization, but also the expansion of bone along the ossification center/suture axis, resulting in either synostosis or open foramina.

From a clinical perspective, disturbances in normal skull ossification result in a number of pathologies with often dramatic consequences for children's health. Premature ossification of one or several sutures of the skull leads to an abnormal skull shape or retarded skull growth (Craniosynostosis, CS). The most common type of CS involves disturbances in the formation of a single suture (simple or non syndromic CS), and its etiology remains

unexplained. Multiple suture synostoses (syndromic CS) are often associated with syndromes of genetic origin i.e. Apert syndrome, Crouzon syndrome, Pfeiffer syndrome and Saethre-Chotzen syndrome [12]. The incidence of non-syndromic CS in United States is about 34.3/100,000 live births while syndromic CS is rare; their incidence is about 1.5/100,000 [13]. The treatment of CS is composed of multiple surgical interventions to correct the abnormal shape of the head, give space for the brain to grow in a normal fashion and prevent the development of intracranial pressure leading to neurological and brain damage complications or death [14]. Complications from surgical treatment can lead to infection, re-ossification, and death from hemorrhage [15].

Cranial osteogenesis and the differentiated state of the bone/suture interface are regulated by extracellular matrix molecules that transmit signals across the cell membrane into the cytoplasm, activating a number of signaling pathways, which subsequently affect gene expression [16],[17]. One of the recently discovered members of the bone extracellular matrix is ameloblastin (AMBn), a glycoprotein previously only associated with the extracellular enamel matrix [18],[19]. Recent studies have noted Ambn expression also in dentin, cementum, pulp, cranial bones, and primary osteoblasts [20–25]. Moreover, Ambn has been shown to regulate *Msx2* expression in ameloblasts [18] [26], and

Msx2 mRNA expression was dysregulated in *Ambn* deficient mice [26]. In the present study, we hypothesized that *Ambn* might affect the growth of craniofacial bones and the patency of cranial sutures through its effect on *Msx2* and possibly other mechanisms. Here we have tested this hypothesis using *Ambn* transgenic mice and *in vitro* models. Our studies reveal a distinct effect of *Ambn* on craniofacial bone growth and suture closure, and suggests possible mechanisms of action.

Materials and Methods

Transgene constructs and transgenic mice

Two transgenic constructs were generated using a modified pSKII-trans vector in which the *K14* promoter, the polyA signal (a generous gift from Dr. Elaine Fuchs, Rockefeller University), the β -globulin intron, the mouse *Ambn* coding region, or the *LacZ* gene was inserted. The β -globulin intron was used to ensure that the transgenes were transcribed properly. The transgenic fragments were freed from pSKII-K14-AMBN or pSKII-K14-LacZ by digesting the constructs with Sac I and Hind III, gel purified and microinjected into mouse zygotes [19]. Mice used in the present study included human keratin 14 (*K14*) promoter-driven *Ambn* transgenic mice (*Ambn*Tg, E18.5, P1, 20, 35 and 60 days of age, $n = 14$) and *K14* promoter-driven *LacZ* transgenic mice (P1, $n = 3$). This study was carried out in strict accordance with the recommendations in the Guide for the Care and Use of Laboratory Animals of the National Institutes of Health. The protocol was approved by the Committee on the Ethics of Animal Experiments of the University of Illinois at Chicago (Permit Number: 11-077). For further analysis, mice were euthanized in a CO₂ chamber followed by cervical dislocation, and calvarial bone and suture tissues were collected for fixation or RNA/protein extraction.

Genotyping. Genotyping was carried out using tails collected from *Ambn*Tg or *LacZ* transgenic heterozygous litters [19]. The tails were lysed in DirectPCR (Tail) buffer (Viagen, Los Angeles, CA) at 50°C overnight and then 85°C for 40 min. PCR was performed using a set of specific primers for *K14* promoters: a forward primer 5'GCTTAGCCAGGGTGACAGAG 3' and a reverse primer 5'CACAGAGGCGTAAATGCAGA3'. After 35 reaction cycles, aliquots of the PCR products were separated on a 2.0% TAE (Tris acetate EDTA) agarose gel, stained with ethidium bromide, and photographed under UV light [19].

Table 1. Primer sequences for RT-PCR analysis.

AMBN	5' aaaaccaccaacacctgag	3' cattgtctccccgagatattg
β -ACTIN	5' gatcattgtctctctgagc	3' acatctgtctggaaggtggac
IBSP	5' gaagcaggtgcagaaggaac	3' gaaaccggttcagaaggaca
CCND1	5' cacacggactacaggggagt	3' cgcggagtctgtagctctct
Coll A	5' caccctcaagagcctgagtc	3' tccgctcttcagctcagagt
MSX2	5' agacatatgagccccaccac	3' caaggctagaagctgggagtg
OCN	5' tcgtgtgtctctccacagc	3' tggccacttaccacaaggtag
OPN	5' ttccaagagagaccaggaga	3' ttgtggctctgatgtccag
OSX	5' cccctgttcttcacagcttc	3' gggaaaacggcaaatagtag
RunX2	5' ccaccactcactaccacacg	3' tatggagtgtctgtctgtctg

doi:10.1371/journal.pone.0052800.t001

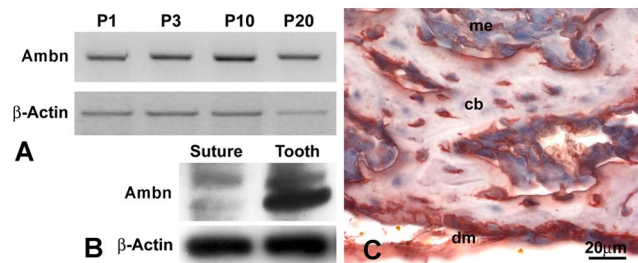


Figure 1. *Ambn* expression in cranial bone and dura mater. (A) RT-PCR analysis of *Ambn* mRNA expression in the posterior frontal suture region from 1, 3, 10, and 20 days postnatal WT mice. The β -Actin gene was used as internal control. (B) Western blot analysis of AMBN protein expression in postnatal day 3 posterior-frontal (PF) suture tissues and teeth. Two bands at 55 and 50 kDa were recognized. β -Actin was used as loading reference. (C) Immunostained sections of cranial bone and dura mater from 3 day postnatal wildtype (WT) mice demonstrated *Ambn* protein localization in calvarial bone (cb), dura mater (dm), and condensed mesenchymal cells (me). Note the high levels of *Ambn* protein in the dura mater and in calvarial osteoblasts. Bar = 20 μ m.
doi:10.1371/journal.pone.0052800.g001

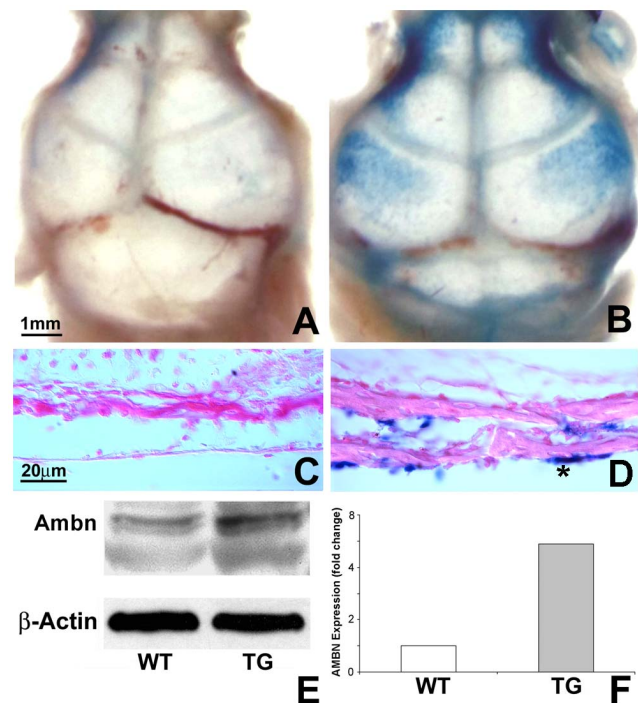


Figure 2. *LacZ* and *Ambn* transgene expression in cranial bone and sutures. (A and B) Whole mount β -gal staining of wildtype (WT) and *K14-LacZ* overexpressing mouse skulls. The β -gal blue signal was localized in cranial bones and sutures of the *Ambn* overexpressor. (C and D) Histological sections of β -gal stained and Eosin counterstained skulls were prepared from the coronal plane of the calvaria in the posterior-frontal region. Note the β -gal positive calvarial osteoblasts in the *Ambn* transgenic mouse sections. No blue staining of β -gal was detected in the WT skull section. Bar for A and B = 1 mm, C and D = 20 μ m. (E) Western blot analysis of protein extracts from WT and *Ambn* transgenic calvarial bone and sutures at age postnatal day 3. The *Ambn* protein level in the transgenic mouse (right lane, upper panel) was 5-fold higher than that in the control mouse (left lane, upper panel) after normalization with β -actin (lower panel).
doi:10.1371/journal.pone.0052800.g002

Dry skull preparation, whole mount X-gal staining and alcian blue/alizarin red staining

Dry skulls of three adult mice from wild-type and *Ambn* transgenic mice at postnatal day 60 ($n=3$) were prepared using *Dermestes* beetles. Briefly, the crude muscle and soft tissues were removed from the animal heads and left cool-dry for several days. The dry skulls were gently placed in a container with *Dermestes* beetles for several days at 30°C under close observation. Once the soft tissues of skulls were completely removed, the dry skulls were collected and cleaned meticulously with a soft brush. The dry skull, and especially the cranial suture of each animal was examined and photographed under a stereo microscope. Width of the posterior frontal suture of each animal was measured with a digital caliper and recorded in mm units. For whole mount X-gal staining, de-skinned animal heads were fixed with 4% paraformaldehyde in PBS at 4°C overnight. The samples were rinsed with PBS at room temperature 3 times for 15 minutes each and then incubated in the dark with a staining buffer containing 0.05 mM $K_3Fe(CN)_6$, 0.05 mM $K_4Fe(CN)_6$, 1 mM $MgCl_2$ and 1 mg/ml X-gal at 37°C for 7 hours. For whole mount alcian blue/alizarin red staining, three embryos from the wild type and *Ambn* transgenic groups at embryonic day 18.5 ($n=3$) were fixed and dehydrated with 70%, 100% ethanol and acetone. The samples were stained with saturated alcian blue (Sigma, St Louis, MO) in 95% ethanol for 2 days, destained with 95% ethanol, and rehydrated. Subsequently, samples were then stained with saturated alizarin red S (Sigma) in 0.5% potassium hydroxide (KOH) solution for 2 days,

destained in 0.5% KOH solution until all soft connective tissue turned clear and then stored in 80% glycerol.

Tissue processing

Calvaria and cranial sutures from wildtype, *Ambn* or *LacZ* transgenic mice at age of embryonic 18 and postnatal 35 days ($n=3$) were dissected and fixed with 10% formalin at 4°C and demineralized in a solution containing 45% EDTA, 4.5% NaOH and 1% formalin at 4°C until the demineralization was completed. The demineralized samples were embedded in paraffin, cut in 5 μ m sagittal sections and mounted on glass slides. Thereafter, the samples were deparaffinized, rehydrated, and stained with Hematoxylin and Eosin or subjected to immunohistochemistry.

Immunohistochemistry

Sections were deparaffinized, rehydrated, and treated with 6% peroxide and methanol followed by a brief incubation in 10 mM sodium citrate buffer with 0.05% Tween 20 at pH 6.0 for antigen retrieval. Sections were then incubated in 2% bovine serum albumin (BSA) for 30 minutes at room temperature to block nonspecific binding of the antibody. After blocking, sections were first incubated with affinity purified anti-Ambn antibody [19],[27] at dilution of 1:200, and then with anti-rabbit secondary antibody (Abcam, Cambridge, MA) at dilution of 1:2000. The expression of Ambn protein was visualized with a Histomouse Broad Spectrum AEC kit (Invitrogen, Carlsbad, CA) under a light microscope. As a negative control, non-immune rabbit serum was used instead of the primary antibody.

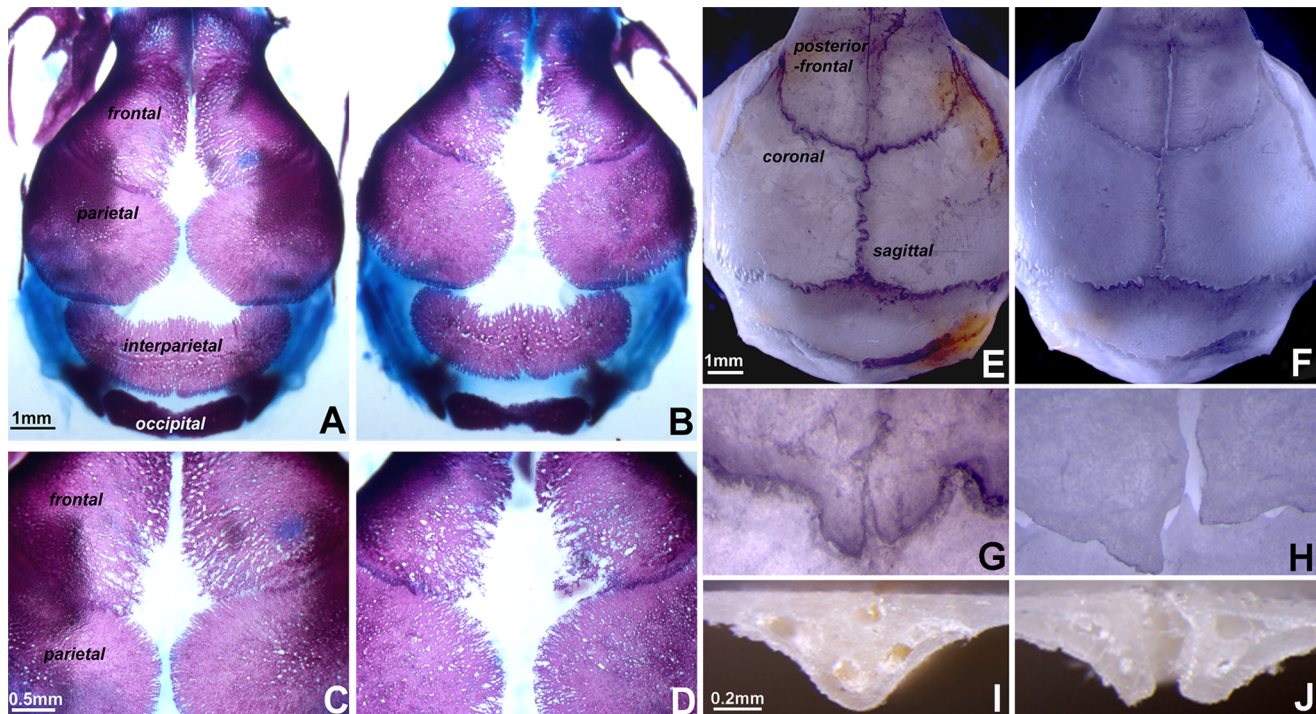


Figure 3. Delayed posterior frontal suture closure in *Ambn* overexpressing mice. (A and B) Whole mount alcian blue/alizarin red staining of wildtype (WT) (A) and *Ambn* transgenic (TG) (B) animals at embryonic stage day 18. The interfrontal gap was wider in the transgenic skulls compared to controls. (C and D) Higher magnification of the skulls shown in A and B. Note that the margins of the frontal bone osteogenic front were not well defined, and the interfrontal and parietal spaces were wider in transgenic mice compared to controls. (E and F) Dried skulls of WT and TG animals at 35 days postnatal. The PF suture was closed in WT mice (E), but remained patent in transgenic mice (F). (G and H) Higher magnification of the skulls shown in A and B. In TG mice, sutures remained open and adjacent bones overlapped (H). Cross-sections of the PF suture revealed the ossified areas of WT mice (I) and TG mice (J) at age 35 day postnatal. The PF suture was sealed by ossification in WT mice, while the left and right parietal bones were linked by soft tissue in TG mice. doi:10.1371/journal.pone.0052800.g003

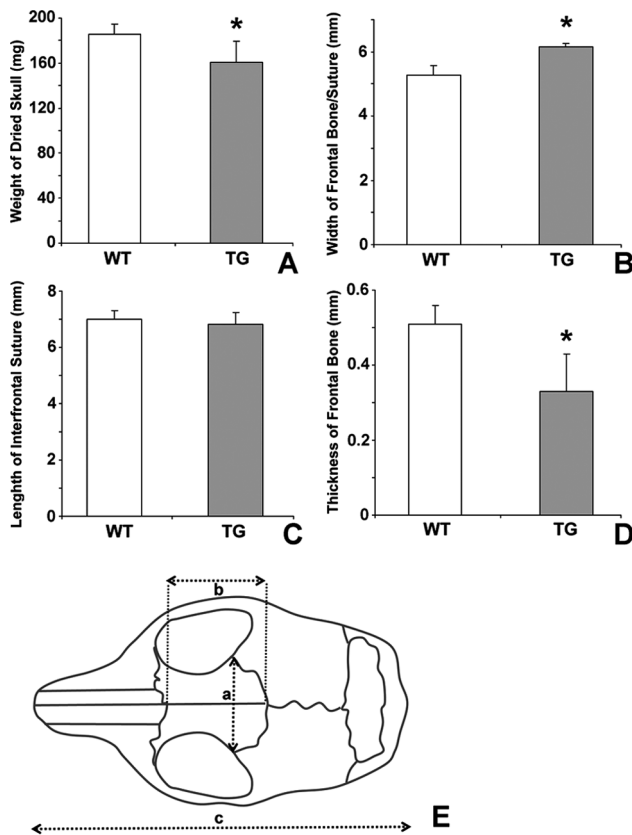


Figure 4. Weight and size comparison between wildtype and *Ambn* transgenic mice dried skulls. Dried skulls were prepared from 60 days postnatal wildtype (WT) and *Ambn* transgenic (TG) mice. Weight of dried skulls (A), width of frontal bone and suture (B), length of interfrontal suture (C) and thickness of frontal bone (D) were measured, and values were graphed as mean \pm standard deviation (SD). * represents significant difference, $p < 0.05$ (Kruskal-Wallis one-way analysis). (E) Anatomical reference points for skull morphological measurements, including width of frontal bone and suture (a), length of interfrontal suture (b), and overall skull length (c). doi:10.1371/journal.pone.0052800.g004

BrdU and TUNEL staining

For BrdU staining, pregnant mice at E18 were injected with BrdU (100 mg/kg) intraperitoneally prior to euthanization. Calvaria and cranial sutures were dissected and processed for paraffin sections. The sections were deparaffinated, rehydrated, and stained with biotinylated anti-BrdU antibody. The BrdU positive cells were detected with the streptavidine-biotin system (Invitrogen). For TUNEL staining, sections were first exposed to proteinase K (20 μ g/ml) at ambient temperature for 10 min, and then incubated with TdT staining solution at 37°C for 1 hour according to the manufacturer's instruction (Promega, Madison, WI). The fluorescence-dUTP-labeled DNA was visualized using a fluorescence microscope.

Cell Culture

The mouse suture mesenchymal cells were isolated from the underlying dura mater and overlying pericranium of posterior frontal and sagittal sutures of wildtype and *Ambn* transgenic mice at postnatal 3 days, and maintained in α -minimum essential medium supplemented with 10% fetal bovine serum, 100 U/ml penicillin, 100 μ g/ml streptomycin and 25 ng/ml Amphotericin B in a 5% CO₂ atmosphere at 37°C. The medium was changed twice a

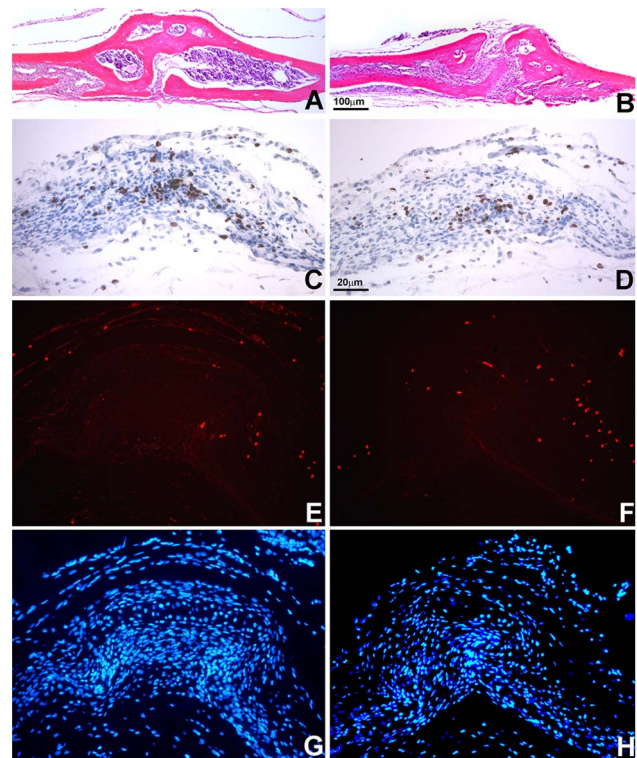


Figure 5. Role of *Ambn* in suture development. (A and B) Cross-sections of the PF suture revealed the ossified areas of wildtype (WT) and *Ambn* transgenic (TG) mice at age of 35 days postnatal. The PF suture was fused by ossification in WT mice (A), while the left and right parietal bones were interrupted by soft tissue in TG mice (B). (C and D) BrdU labeling of proliferative cells in developing sutures. Note the accumulation of BrdU-labeled cells in the suture center of WT mice (C) compared to TG mice (D). (E and F) TUNEL staining in developing sutures. Note the red labeling for TUNEL-positive cells in WT and TG mice. (G and H) DAPI counterstaining of (E and F). doi:10.1371/journal.pone.0052800.g005

week. To study the effects of *Ambn* on cell proliferation and differentiation, suture mesenchymal cells from wildtype and *Ambn* transgenic mice were subjected to regular culture medium or a mineralization induction medium containing 50 μ g/ml ascorbic acid and 2 mM β -glycerophosphate, and cultured for 2–21 days. Upon terminating the culture, cells were used for MTT assay, alkaline phosphatase activity test, alizarin red staining, or RNA and protein preparation.

Alkaline phosphatase and in vitro mineralization assay

After 7 days of culture in osteogenic media, cells were washed and stained with alkaline phosphatase substrate (Roche Diagnostic, Indianapolis, IN) to verify early osteogenic activity. After 21 days of culture in osteogenic media, the cells were fixed with methanol, stained with 10% alizarin red solution, and mineralized nodules were identified as red spots on the culture dish.

Cell proliferation assay

Prior to termination of culture, cells were incubated in MTT solution (2 mg/ml of MTT in DMEM with 2% FBS) for 4 hours. To quantify proliferative activity, the MTT stained cells were lysed in HCL/Isopropanol, and the absorbance was detected at 570 nm with background subtraction at 630 nm [28].

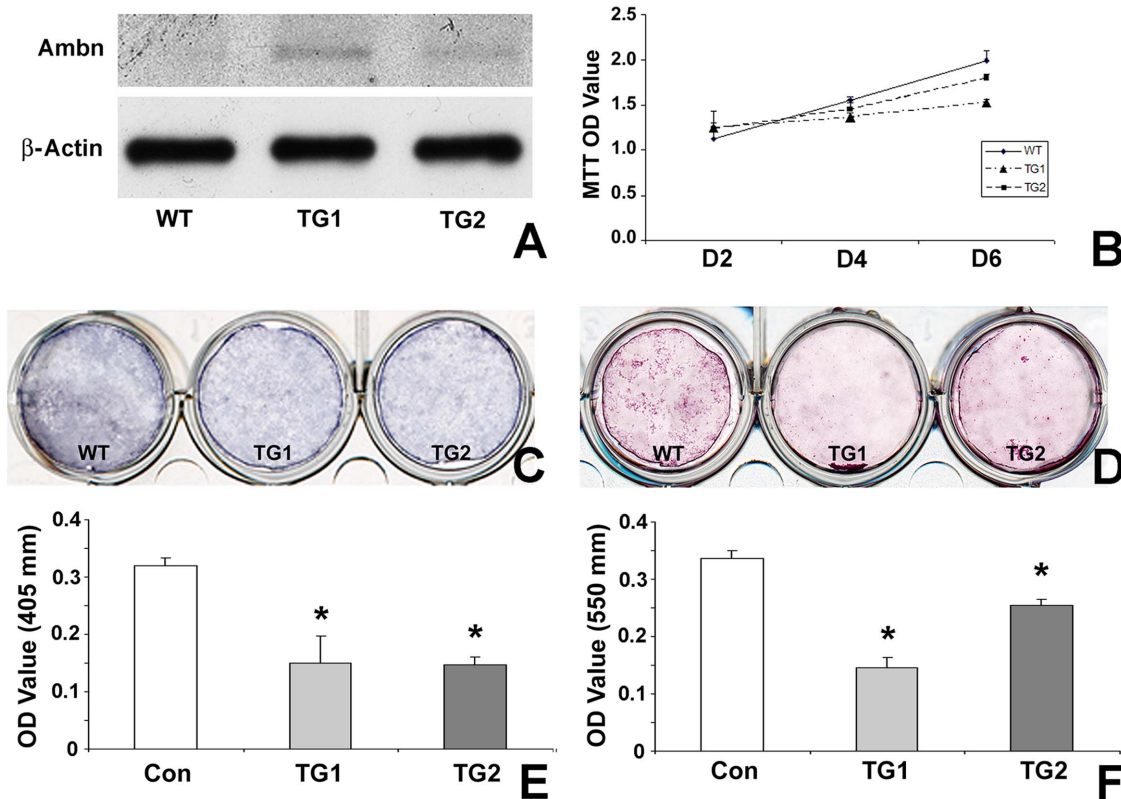


Figure 6. Effect of Ambn on proliferation and differentiation of suture mesenchymal cells. In this study, mesenchymal cells from wildtype (WT) mice and *Ambn* overexpressor (TG) sutures were cultured in osteogenic induction medium. (A) Ambn protein expression in suture-derived cells. β -Actin was used as loading control. (B) MTT assay to compare cell proliferation in WT and TG mesenchymal suture cells. The measured absorbance (mean \pm SD) is proportionate to the number of living cells. (C) Alkaline phosphatase activity staining at day 6 of culture identified differentiated cells positive for alkaline phosphatase with blue staining. (D) Alizarin red staining for mineral nodule formation. Cells were cultured for 21 days in osteogenic induction medium. Mineral nodules were stained in red. All experiments were carried out in triplicate and repeated three times. * represents significant difference, $p < 0.05$ (Kruskal-Wallis one-way analysis). doi:10.1371/journal.pone.0052800.g006

RNA extraction and RT-real time PCR

Total RNAs were isolated from mouse suture tissues or cultured cells using the TRIZOL LS Reagent (Invitrogen) according to the manufacturer's instructions. Two micrograms of total extracted RNA was applied toward cDNA generation with the Sprint RT Complete kit[®] (Clontech, Mountain View, CA). To quantify the mRNA expression levels of transcription factors and bone marker genes, real-time PCR primers were designed based on EMBL/GenBank searches (shown in Table I). Real-time PCR was performed using sequence specific sybergreen primers and the ABI Prism 7000 Sequence detection system (Applied Biosystems, Foster City, CA). Reaction conditions were as follows: 2 min at 50°C (one cycle), 10 min at 95°C (one cycle), and 15 sec at 95°C, and 1 min at 60°C (40 cycles). Samples were normalized using GAPDH. The analyses were performed in triplicate for three independent experiments to confirm reproducibility of the results. Relative expression levels were calculated using the $2^{-\Delta\Delta Ct}$ method [29], and values were graphed as the mean expression level \pm standard deviation.

Protein extraction and western blot analysis

Calvaria from 3 transgenic and 3 control animals at age P20 were collected and homogenized under liquid N₂. Equal amounts of protein extracts in a lysis buffer containing 100 mM Tris HCl pH 9.0, 200 mM KCl, 25 mM EGTA, 36 mM MgCl₂, 2% deoxycholic acid and 10% DTT v/v were subjected to SDS-

polyacrylamide gel electrophoresis (Biorad, Hercules, CA), and the separated proteins were transferred to a PVDF (Polyvinylidene Difluoride) membrane (Immobilon P[®], Millipore, Billerica, MA). The membrane was incubated with rabbit anti-mouse Ambn [19],[27], Msx2, or CcnD1 antibodies (Abcam). Immune complexes were detected with goat anti-rabbit IgG horseradish peroxidase-conjugated secondary antibody (Molecular Probes[®], Carlsbad, CA) and enhanced chemiluminescence reagents (Pierce Biotechnology, Rockford, IL). The amount of protein expression was compared after normalization with the amount of β -actin as an internal calibrator in each lane.

Statistical analysis

Quantitative data were presented as means \pm SD from three independent experiments and compared using Kruskal-Wallis one-way analysis of variance. The difference between groups was considered statistically significant at $P < 0.05$.

Results

AMBn is expressed in calvarial bone

Previous studies have demonstrated that the extracellular matrix protein Ambn is expressed in cranial tissues including enamel [30], cementoblasts [22], and cranial bones [24]. To examine the function of Ambn in cranial bone and suture formation, Ambn expression in mouse posterior frontal suture structures was

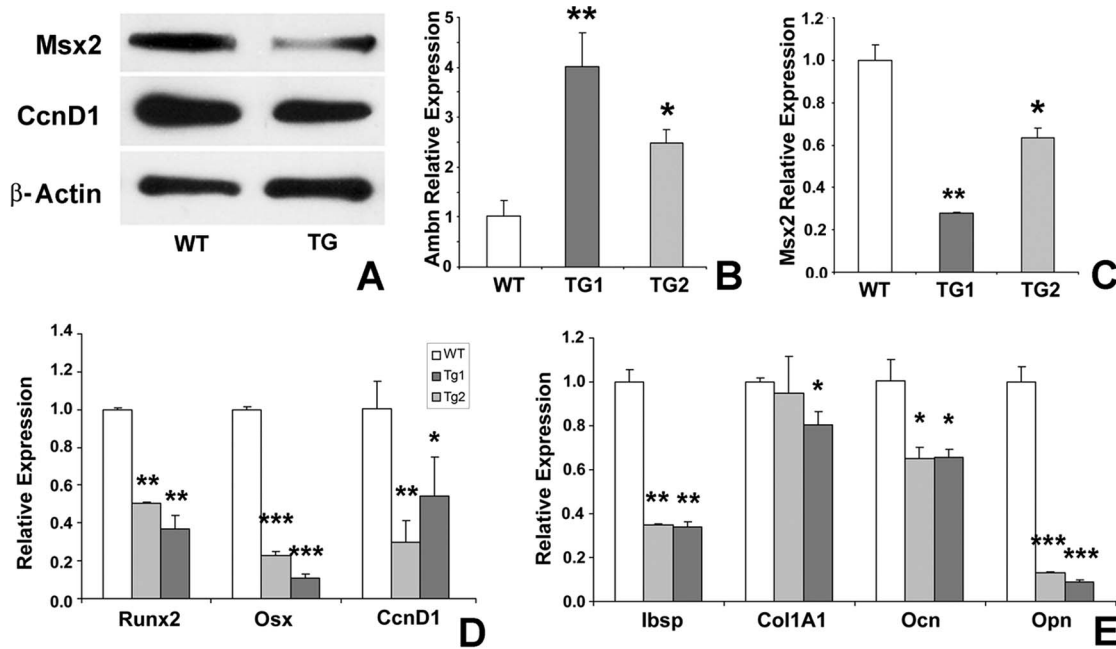


Figure 7. Expression of *Msx2* and downstream genes in suture and suture-derived mesenchymal cells of wildtype and *Ambn* transgenic mice. (A) Western blot analysis of *Msx2* and *CcnD1* expression in sutures. Suture extracts from wildtype (WT) and *Ambn* transgenic (TG) mice were processed for immunoblotting with antibodies against *Msx2* and *CcnD1*. β -Actin was detected as a loading control. (B and C) Quantitative RT real time PCR analysis of *Ambn* (B) and *Msx2* (C) gene expression in suture-derived mesenchymal cells. (D and E) Quantitative RT real time PCR for *Msx2* downstream target genes in cultured mesenchymal suture cells from WT and TG mice; (E) *Runx2*, *Osterix* (*Osx*), and *Cyclin D1* (*CcnD1*) transcription factors; and (F) Bone sialoprotein (*Ibsp*), Collagen I (*Col1A1*), Osteocalcin (*Ocn*), and Osteopontin (*Opn*) matrix proteins. Expression levels were calculated relative to GAPDH gene expression levels using the $2^{-\Delta\Delta Ct}$ method, and values were graphed as the mean expression level \pm standard deviation. **, and *** represent significant difference, $p < 0.05$, $p < 0.01$, and $p < 0.001$ respectively (Kruskal-Wallis one-way analysis). doi:10.1371/journal.pone.0052800.g007

characterized. RT-PCR analysis of samples ranging between postnatal days 1–20 revealed *Ambn* mRNA expression in postnatal cranial sutures (Fig. 1A). Western blotting recognized 50 and 55 kDa bands positive for *Ambn* in calvarial bone extracts (Fig. 1B). Using immunohistochemistry, *Ambn* protein was localized in calvarial bone, dura mater, and adjacent condensed mesenchyme (Fig. 1C).

Five-fold AMBN overexpression in a K14-driven transgenic mouse model

Gain of function mice are useful models to mimic syndromes of genetic origin such as suture synostoses (syndromic CS) [31]. We therefore generated *Ambn* transgenic mice using the human *K14* promoter to drive *Ambn* gene expression [19]. In addition, *K14-LacZ* transgenic mice were created to verify the location of the enforced *Ambn* gene expression [19]. Whole mount β -gal staining of the *K14*-driven *LacZ* transgenic skull revealed dark blue staining in parietal, frontal, maxillary, ethmoid and occipital bones and in calvarial sutures (Fig. 2B), when compared to wildtype mice (Fig. 2A). Histological analysis demonstrated β -gal blue staining in calvarial osteoblasts in transgenic mouse sections (Fig. 2D), but not in control mouse sections (Fig. 2C). When compared on western blots and after normalization with β -actin, the amount of *Ambn* protein from calvarial bones and posterior frontal (PF) sutures was 5 times higher in the *Ambn* transgenic mice than in wildtype controls (Figs. 2E and F).

Posterior frontal suture fusion was delayed in *Ambn* transgenic mice

To determine the effect of *Ambn* on cranial suture closure, skulls from *Ambn* transgenic and wildtype mice were compared using alcian blue/alizarin red staining for cartilage and bone mineralized tissue. *Ambn* transgenic mice at embryonic day 18.5 exhibited wider gaps of interfrontal and interparietal spaces (Figs. 3B and D) compared to those of their controls (Figs. 3A and C) ($n = 3$). There was less bone density and ossification along the suture (Fig. 3D), and the osteogenic margins of frontal bones were disorganized and not well defined (Fig. 3D), when compared to the wildtype control (Fig. 3C). This phenotype was indicative of a delayed development of the frontal bones. Skull samples of adult *Ambn* transgenic animals (age 60 days postnatal) revealed the patency of the posterior frontal sutures, revealing spanned gaps between the frontal bones (Figs. 3F and H), while the controls exhibited complete suture closure (Figs. 3E and G). The posterior frontal suture gap width in the *Ambn* transgenic mice was 0.12–0.42 μm (Fig. 3J), compared to 0.02–0.04 μm in controls (Fig. 3I) ($n = 3$).

Ambn overexpressor skulls weighed less, and their interfrontal bones were thinner and wider

To further characterize the phenotypes of *Ambn* transgenic mice, dried skull samples from wildtype and *Ambn* transgenic mice at age of postnatal day 60 were compared, resulting in at least three significant differences. First, there was a significant 13.2% reduction in weight of *Ambn* transgenic skulls compared to WT controls (Fig. 4A). Second, skull width of *Ambn* transgenic animals was 14.3% increased when measured at the interfrontal bone/

coronal suture interface (Figs. 4B). Third, there was a significant 35.3% reduction in interfrontal bone thickness in transgenic mice (Fig. 4D). Interestingly, there was no significant difference in the length of skulls (data not shown), and in the length of the posterior frontal suture, when comparing wildtype and transgenic groups (Fig. 4C).

Incomplete posterior frontal suture closure and reduced proliferation rates in *Ambn* transgenic mice

Histomorphological analysis demonstrated complete closure of the posterior frontal suture in control mice (Fig. 5A) in contrast to incomplete closure in transgenic mice (Fig. 5B). The micrograph was a fused bony bridge formation on the telencephalic aspect of the calvaria in control mice (Fig. 5A), while the frontal bone arch was interrupted by a soft tissue interface in the *Ambn* transgenic mice (Fig. 5B). The interrupting soft tissue extended from the periosteum to the dura mater in vertical direction (Fig. 5B). BrdU staining of the developing posterior frontal suture (E18) revealed 29% less proliferating cells in *Ambn* transgenic mice. The number of BrdU positive cells per 0.01 mm² in the control group was 124+/-5.6 while the number in *Ambn* TG was 88+/-2.8. In contrast, the number of TUNEL positive cells was 1.3-fold higher in *Ambn* overexpressors (Figs. 5D and F) when compared to wildtype mice (Figs. 5C and E).

Ambn inhibited mouse suture mesenchymal cell proliferation and differentiation in vitro

To determine how *Ambn* affects suture development, suture mesenchymal cells were isolated from underlying dura mater and overlying pericranium of posterior-frontal sutures of wildtype and transgenic mice. Suture mesenchymal cells from wildtype mice expressed basal *Ambn* protein levels (Fig. 6A), while the cells from two different transgenic mice over-expressed *Ambn* protein at about 4.05(TG1) and 2.5(TG2) times higher levels (Figs. 6A and 7B). To further examine whether *Ambn* expression levels affect cell function, proliferation of suture mesenchymal cells was analyzed using the MTT assay. There was an inverse relationship between *Ambn* expression levels and cell proliferation capacity, with highest MTT OD value in wildtype cells, followed by TG2 and then TG1 cells (Fig. 6B). In addition, there was a substantial reduction in alkaline phosphatase activity and Alizarin red staining in the two cell lines from *Ambn* overexpressor mice, TG1 and TG2 (Figs. 6C and D). Remarkably, the high *Ambn* overexpressing cell line TG1 had a stronger effect on Alizarin red-detected mineralization inhibition than the less *Ambn* overexpressing cell line TG2, suggesting that *Ambn* over-expression inhibited suture mesenchyme osteogenic cell differentiation in a dose-dependent manner (Figs. 6D).

Ambn regulated *Msx2* and downstream gene expression

Ambn overexpressor mice displayed posterior frontal suture patency, a phenotype previously reported in *Msx2* deficient mice [32]. In addition, *Ambn* over-expressing suture mesenchymal cells displayed lower proliferative capacity and delayed differentiation similar to the effects of *Msx2* deficiency on mesenchymal cell function [32]. Therefore, *Msx2* expression in suture tissues as well as suture mesenchymal cells from *Ambn* transgenic and wildtype mice was examined. Western blot analysis revealed that *Msx2* and *CcnD1* expression in calvarial bones and PF suture tissues of *Ambn* transgenic mice were downregulated (Fig. 7A). *Msx2* mRNA expression in suture mesenchymal cells from wildtype and transgenic mice was reverse proportional to *Ambn* mRNA expression, when comparing cells from two different transgenic

lines (Fig. 7B and C). To determine whether *Ambn* affects expression of *Msx2* down-stream target genes, expression levels of osteogenic transcription factors *Runx2* and *Osx*, bone matrix proteins *Ibsp*, *ColI*, *Ocn* and *Opn*, as well as the cell cycle-related gene *CcnD1* were detected using quantitative RT real time PCR. Our data demonstrated that *Ambn* overexpression resulted in significant decreases in bone transcription factor and bone mineralization marker gene expression in a dose-dependent manner (Figs. 7D and E). Similarly, *CcnD1* expression was downregulated in TG1 and TG2 cells. Together, these studies indicate that *Ambn* inhibits cell proliferation and reduces *Msx2* and downstream gene expression *in vivo* and *in vitro*.

Discussion

Transgenic animal models are ideal biological systems to test the effect of forced gene expression on the development of a phenotype. In the present study we have used the human *Keratin 14* promoter to overexpress the extracellular matrix protein *Ambn* in calvarial osteoblasts and suture mesenchymal cells. Keratin 14(K14, Cytokeratin 14 = CK14) is commonly known as an epithelial protein encoded by the *KRT14* gene. However, K14 expression in calvarial osteoblasts has been previously reported and confirmed by Western blot [33]. In addition, reports of keratins in non-epithelial cell lineages have become more frequent in the literature, including mouse studies related to keratins involved in endodermal and mesoderm adhesion in early embryogenesis [34] (Vijayaraj et al. 2010, reports on K19 in dental papilla and dental pulp [35] (Webb et al. 1995), microarray and western blot detection of K18 in cementoblasts [36] (Dangaria et al. 2011), findings of K19 and K8 in mature striated muscle [37] (Shah et al. 2012), and K8 and K18 expression in mesenchymal progenitors of regenerating limbs [38] (Cocoran and Ferretti 1997). Here, *K14* expression in calvarial osteoblasts was further confirmed by β -gal staining for the *K14 LacZ* transgene in *K14 LacZ* transgenic mice using both histology and whole mount staining. The *K14* promoter system has become a promoter of choice in our and other laboratories because of its efficient expression of many transgenes [39],[40]. *K14*-driven overexpression of *Ambn* in mouse calvaria resulted in a robust 5-fold enhancement of *Ambn* levels in calvarial tissue extracts.

Our study indicates that *Ambn* was expressed in developing calvarial bone and sutures. This finding matches other reports of *Ambn* expression during bone formation [25],[41] and expands its original concept as an ameloblast-specific gene product [42]. However, when compared to the developing enamel matrix, expression levels were less, suggesting that *Ambn* may not act directly on bone development by controlling crystal growth as it does in the enamel matrix [29],[43], but rather indirectly as a signaling molecule affecting the expression of transcription factors and extracellular matrix signaling pathways [23],[44],[45]. This concept is supported by findings reported in the present study that already small differences in *Ambn* concentration have significant effects on cell behavior, including cell proliferation and mineralization.

Our human *K14*-driven *Ambn* overexpressor mice suffered from delayed and/or incomplete cranial suture closure and displayed patency of the posterior frontal suture. Moreover, frontal bones of *Ambn* overexpressors weighed less and were thinner, suggestive that *Ambn* was involved in tissue growth or mineralization or both. We interpret these findings to indicate that *Ambn* plays an important role in the growth and development of cranial bones and subsequent suture closure. Our concept that *Ambn* affects mineralized tissues outside of teeth is supported by earlier studies

related to the effect of *Ambn* on bone [41]. In our study, the phenotype of incomplete suture closure in *Ambn* overexpressing mice is explained by two related *in vitro* findings, namely (i) a significant reduction in suture mesenchymal cell proliferation and (ii) a downregulation of the cell proliferation marker cyclin D1 (*CcnD1*). In addition, studies in our and other laboratories have also provided evidence for the inhibitory effect of *Ambn* on cell proliferation, e.g. an increase of the cell proliferation inhibitors p21 and p27 in *Ambn* overexpressing ameloblasts [26],[46]. In contrast, there have also been reports suggesting that *Ambn* promotes bone healing by enhancing progenitor cell proliferation [41] (Tambursten et al. 2011) and regulates osteogenic differentiation [47] (Iizuku et al.). We propose that such findings may be due to different concentrations of *Ambn* acting either as a signaling molecule or a structural matrix protein [48] (Diekwisch 2011).

Another factor responsible for the inhibition of suture closure by *Ambn* overexpression is the transcription factor *Msx2*, a causative gene involved in human cranial suture pathologies such as CS and EPF [49],[50]. Our finding that *Msx2* is downregulated by *Ambn* is supported by earlier studies reporting upregulation of *Msx2* in ameloblasts from *Ambn* deficient mice [19] and downregulation of *MSX2* in human ameloblastoma cells overexpressing *AMBN* [26]. Notably, *Msx2* deficient mice featured a patency of the posterior frontal suture [32], a phenotype resembling the *Ambn* overexpressor phenotype described in the present study. Underscoring the severe clinical impact of defects caused by changes in *Msx* levels and suture development, *Msx1/2* double mutant embryos were lacking frontal bones and died at E17 to E18 [51]. Together, these studies indicate that changes in *Ambn* affect craniofacial growth and suture closure via *Msx2*.

Evidence from previous studies suggests that the effects of *Ambn* on *Msx2* suppression and calvarial osteoblast proliferation inhibition may be related, as it has been shown that *Msx2* increases the expression of *CcnD1*, inhibits cell differentiation [52], and influences the number of proliferative osteogenic cells in growth centers of the developing mouse skull [53]. Others have reported that calvarial osteoblasts derived from *Msx2* deficient mice had a lower rate of proliferation and demonstrated accelerated osteoblastic differentiation at a later stage when compared to osteoblasts derived from wildtype mice [54]. Our finding that suture mesenchymal cells from transgenic mice reduced *CcnD1* and osteogenic gene expression under subconfluent condition supported a potential connection between the role of *Ambn* in osteogenic differentiation and its role in cell proliferation inhibition. Together, our data indicate that *Ambn* affects calvarial osteoblast proliferation and differentiation through suppression of the transcription factor *Msx2*.

Conclusions

These data suggested that the extracellular matrix protein *Ambn* plays a crucial role in cranial suture closure. The effect of *Ambn* on suture closure may be explained by the inhibitory effect of *Ambn* on the transcription factor *Msx2* and its effect on cell proliferation, resulting in reduced growth and differentiation of calvarial osteoblasts as well as delayed suture closure in mice.

Author Contributions

Conceived and designed the experiments: X.Luan. Performed the experiments: PA YI X.Lu YZ. Analyzed the data: PA X.Lu. Wrote the paper: PA CE X.Luan.

References

- Bruce JA (1941) Time and order of appearance of ossification centers and their development in the skull of the rabbit. *Am J Anat* 68: 41–67.
- Hall BK (2005) *Bones and Cartilage: development skeleton biology*. San Diego: Academic press. 760p.
- Ornitz DM, Marie PJ (2002) FGF signaling pathways in endochondral and intramembranous bone development and human genetic disease. *Genes Dev* 16: 1446–1465.
- Komori T, Yagi H, Nomura S, Yamaguchi A, Sasaki K, et al. (1997) Targeted disruption of *Cbfa1* results in a complete lack of bone formation owing to maturational arrest of osteoblasts. *Cell* 89: 755–764.
- Lee B, Thirunavukkarasu K, Zhou L, Pastore L, Baldini A, et al. (1997) Missense mutations abolishing DNA binding of the osteoblast-specific transcription factor *OSF2/CBFA1* in cleidocranial dysplasia. *Nat Genet* 16: 307–310.
- Mundlos S, Otto F, Mundlos C, Mulliken JB, Aylsworth AS, et al. (1997) Mutations involving the transcription factor *CBFA1* cause cleidocranial dysplasia. *Cell* 89: 773–779.
- Dodig M, Tadic T, Kronenberg MS, Dacic S, Liu YH, et al. (1999) Ectopic *Msx2* overexpression inhibits and *Msx2* antisense stimulates calvarial osteoblast differentiation. *Dev Biol* 209: 298–307.
- el Ghouzzi V, Le Merrer M, Perrin-Schmitt F, Lajeunie E, Benit P, et al. (1997) Mutations of the *TWIST* gene in the Saethre-Chotzen syndrome. *Nat Genet* 15: 42–46.
- Howard TD, Paznekas WA, Green ED, Chiang LC, Ma N, et al. (1997) Mutations in *TWIST*, a basic helix-loop-helix transcription factor, in Saethre-Chotzen syndrome. *Nat Genet* 15: 36–41.
- Kopher RA, Mao JJ (2003) Suture growth modulated by the oscillatory component of micromechanical strain. *J Bone Miner Res* 18: 521–528.
- Opperman LA, Rawlins JT (2005) The extracellular matrix environment in suture morphogenesis and growth. *Cells Tissues Organs* 181: 127–135.
- Rice DP (2008) Clinical features of syndromic craniosynostosis. *Front Oral Biol* 12: 91–106.
- Cohen MJ, Maclean R (2000) *Craniosynostosis, diagnosis, evaluation, and management*. Oxford: Oxford University Press. 727p.
- Hukki J, Saarinen P, Kangasniemi M (2008) Single suture craniosynostosis: Diagnosis and imaging. In: Rice DP, editor. *Craniofacial sutures. Development, disease and treatment*. *Front Oral Biol* 12: 79–90.
- Whitaker LA, Munro IR, Salyer KE, Jackson IT, Ortiz-Monasterio F, et al. (1979) Combined report of problems and complications in 793 craniofacial operations. *Plast Reconstr Surg* 64: 198–203.
- Adams JC, Watt FM (1993) Regulation of development and differentiation by the extracellular matrix. *Development* 117: 1183–1198.
- Carinci P, Becchetti E, Bodo M (2000) Role of the extracellular matrix and growth factors in skull morphogenesis and in the pathogenesis of craniosynostosis. *Int J Dev Biol* 44: 715–723.
- Fukumoto S, Kiba T, Hall B, Iehara N, Nakamura T, et al. (2004) Ameloblastin is a cell adhesion molecule required for maintaining the differentiation state of ameloblasts. *J Cell Biol* 167: 973–983.
- Lu X, Ito Y, Kulkarni A, Gibson C, Luan X, et al. (2011) Ameloblastin-rich enamel matrix favors short and randomly oriented apatite crystals. *Eur J Oral Sci* 119 Suppl: 254–260.
- Fong CD, Cerny R, Hammarstrom L, Slaby I (1998) Sequential expression of an amelin gene in mesenchymal and epithelial cells during odontogenesis in rats. *Eur J Oral Sci* 106 Suppl: 324–330.
- Hao J, He G, Narayanan K, Zou B, Lin L, et al. (2005) Identification of differentially expressed cDNA transcripts from a rat odontoblast cell line. *Bone* 37: 578–588.
- Nunez J, Sanz M, Hoz-Rodriguez L, Zeichner-David M, Arzate H (2010) Human cementoblasts express enamel-associated molecules *in vitro* and *in vivo*. *J Periodontol Res* 45: 809–814.
- Spahr A, Lyngstadaas SP, Slaby I, Haller B, Boeckh C, et al. (2002) Expression of amelin and trauma-induced dentin formation. *Clin Oral Investig* 6: 51–57.
- Spahr A, Lyngstadaas SP, Slaby I, Pezeshki G (2006) Ameloblastin expression during craniofacial bone formation in rats. *Eur J Oral Sci* 114: 504–511.
- Tambursten MV, Rescand JE, Spahr A, Brookes SJ, Kvalheim G, et al. (2010) Ameloblastin expression and putative autoregulation in mesenchymal cells suggest a role in early bone formation and repair. *Bone* 48: 406–413.
- Sonoda A, Iwamoto T, Nakamura T, Fukumoto E, Yoshizaki K, et al. (2009) Critical role of heparin binding domains of ameloblastin for dental epithelium cell adhesion and ameloblastoma proliferation. *J Biol Chem* 284: 27176–27184.
- Zhang X, Diekwisch TGH, Luan X (2011) structure and function of ameloblastin as an extracellular matrix protein: adhesion, calcium binding, and CD63 interaction in human and mouse. *Eur J Oral Sci* 119 Suppl: 270–279.
- Loveland BE, Johns TG, Mackay IR, Vaillant F, Wang ZX, et al. (1992) Validation of the MTT dye assay for enumeration of cells in proliferative and antiproliferative assays. *Biochem Int* 27: 501–510.
- Livak KJ, Schmittgen TD (2001) Analysis of relative gene expression data using real-time quantitative PCR and the 2⁻(Delta Delta C(T)) Method. *Methods* 25: 402–408.

30. Lee SK, Krebsbach PH, Matsuki Y, Nanci A, Yamada KM, et al. (1996) Ameloblastin expression in rat incisors and human tooth germs. *Int J Dev Biol* 40: 1141–1150.
31. Shen K, Krakora SM, Cunningham M, Singh M, Wang X, et al. (2009) Medical treatment of craniosynostosis: recombination Noggin inhibits coronal suture closure in the rat craniosynostosis model. *Orthod Craniofac Res* 12: 254–262.
32. Satokata I, Ma L, Ohshima H, Bei M, Woo I, et al. (2000) *Msx2* deficiency in mice causes pleiotropic defects in bone growth and ectodermal organ formation. *Nat Genet* 24: 391–395.
33. Kumar A, Singh AK, Gautam AK, Chandra D, Singh D, et al. (2010) Identification of kaempferol-regulated proteins in rat calvarial osteoblasts during mineralization by proteomics. *Proteomics* 10: 1730–1739.
34. Vijayaraj P, Kroeger C, Reuter U, Hartmann D, Magin TM (2010) Keratins regulate yolk sac hematopoiesis and vasculogenesis through reduced BMP-4 signaling. *Eru J Cell Biol* 89: 299–306.
35. Webb PP, Moxham BJ, Ralphs JR, Benjamin M (1995) Cytoskeleton of the mesenchymal cells of the rat dental papilla and dental pulp. *Connect Tissue Res* 32: 71–76.
36. Dangaria S, Ito Y, Luan X, Diekwisch TG (2011) Differentiation of neural-crest-derived intermediate pluripotent progenitors into committed periodontal populations involves unique molecular signature changes, cohort shifts, and epigenetic modifications. *Stem Cell Dev* 20: 39–52.
37. Shah SB, Love JM, O'Neill A, Lovering RM, Bloch RJ (2012) Influences of desmin and keratin 19 on passive biomechanical properties of mouse skeletal muscle. *J Biomed Biotech* doi:10.1155/2012/704061.
38. Corcoran JP, Ferretti P (1997) Keratin 8 and 18 expression in mesenchymal progenitor cells of regenerating limbs is associated with cell proliferation and differentiation. *Dev Dyn* 210: 355–370.
39. Wang X, Zinkel S, Polonsky K, Fuchs E (1997) Transgenic studies with a keratin promoter-driven growth hormone transgene: prospects for gene therapy. *Proc Natl Acad Sci U S A* 94: 219–226.
40. Luan X, Ito Y, Diekwisch TG (2006) Evolution and development of Hertwig's epithelial root sheath. *Dev Dyn* 235: 1167–1180.
41. Tamburset MV, Reppe S, Spahr A, Sabetrsek R, Kvalheim G, et al. (2010) Ameloblastin promotes bone growth by enhancing proliferation of progenitor cells and by stimulating immunoregulators. *Eur J Oral Sci* 118: 451–459.
42. Krebsbach PH, Lee SK, Matsuki Y, Kozak CA, Yamada KM, et al. (1996) Full-length sequence, localization, and chromosomal mapping of ameloblastin. A novel tooth-specific gene. *J Biol Chem* 271: 4431–4435.
43. Lee SK, Kim SM, Lee YJ, Yamada KM, Yamada Y, et al. (2003) The structure of the rat ameloblastin gene and its expression in amelogenesis. *Mol Cells* 15: 216–225.
44. Fukumoto S, Yamada A, Nonaka K, Yamada Y (2005) Essential roles of ameloblastin in maintaining ameloblast differentiation and enamel formation. *Cells Tissues Organs* 181: 189–195.
45. Wazen RM, Moffatt P, Zalzal SF, Yamada Y, Nanci A (2009) A mouse model expressing a truncated form of ameloblastin exhibits dental and junctional epithelium defects. *Matrix Biol* 28: 292–303.
46. Zhang Y, Zhang X, Lu X, Atsawasuwan P, Luan X (2011) Ameloblastin regulate cell attachment and proliferation through RhoA and p27. *Eur J Oral Sci* 119 Suppl: 280–285.
47. Iizuka S, Kudo Y, Yoshida M, Tsunematsu T, Yoshiko Y, et al. (2011) Ameloblastin regulates osteogenic differentiation by inhibiting Src kinase via cross talk between integrin β 1 and CD63. *Mol Cell Biol* 31: 783–792.
48. Diekwisch T (2011) Evolution and ameloblastin. *J Eur Oral Sci* 119 Suppl: 293–297.
49. Jabs EW, Muller U, Li X, Ma L, Luo W, et al. (1993) A mutation in the homeodomain of the human *MSX2* gene in a family affected with autosomal dominant craniosynostosis. *Cell* 75: 443–450.
50. Wilkie AO, Tang Z, Elanko N, Walsh S, Twigg SR, et al. (2000) Functional haploinsufficiency of the human homeobox gene *MSX2* causes defects in skull ossification. *Nat Genet* 24: 387–390.
51. Han J, Ishii M, Bringas P Jr, Maas RL, Maxson RE Jr, et al. (2007) Concerted action of *Msx1* and *Msx2* in regulating cranial neural crest cell differentiation during frontal bone development. *Mech Dev* 124: 729–745.
52. Hu G, Lee H, Price SM, Shen MM, Abate-Shen C (2001) *Msx* homeobox genes inhibit differentiation through upregulation of cyclin D1. *Development* 128: 2373–2384.
53. Liu YH, Tang Z, Kundu RK, Wu L, Luo W, et al. (1999) *Msx2* gene dosage influences the number of proliferative osteogenic cells in growth centers of the developing murine skull: a possible mechanism for *MSX2*-mediated craniosynostosis in humans. *Dev Biol* 205: 260–274.
54. Marjanovic I, Kronenberg MS, Erceg I, Lichter AC (2009) Comparison of proliferation and differentiation of calvarial osteoblast cultures derived from *Msx2* deficient and wild type mice. *Coll Antropol* 33: 919–924.